WASHINGTON STATE DEPARTMENT OF
Natural Resources
Peter Goldmark - Commissioner of Public Lands
Division of Geology and Earth Resources
David K. Norman - State Geologist

Geophysical, Stratigraphic, and Structural Analyses of the Snoqualmie 7.5-minute Quadrangle, King County, Washington

TERTIARY TO QUATERNARY DEFORMATION IN THE MAP AREA—FAULTS, BASINS, AND FOLDS

Tertiary to recent deformation of the study area has resulted in basins that are bounded by strike-slip to oblique-slip faults, although some faults with a significant vertical component of slip are mapped in the northeastern part of the area. The basins are located within the broad Rattlesnake Mountain fault zone (RMFZ), a regional strike-slip fault zone that likely correlates with the Southern Whidbey Island fault (SWIF), northwest of the map area (Fig. 1, site 3; Sherrod and others, 2008; Dragovich and others, 2007). The RMFZ likely merges with the Olympic–Wallowa lineament south of the map area and truncates the Seattle fault zone west of the map area (Fig. 1, sites 1 and 7). The Miocene volcanic rocks of Snoqualmie Falls are preserved in one of these fault-controlled basins. Some Quaternary basins within the RMFZ are both modeled as inverted sedimentary basins that are shortened and uplifted former extensional basins. Basin inversion is facilitated by compressional reactivation of extensional faults and generates a distinctive deformational architecture. The thick accumulations of Quaternary sediments in the North Bend, Snoqualmie Valley, and Snoqualmie basins (Figs. 1 and 2) are suggestive of ongoing extension. However, the older Olympia beds on Snoqualmie Ridge provide the best example of an inverted basin. These exceptionally thick beds of ancient Snoqualmie River alluvium are elevated, folded, and faulted within the RMFZ. There are other possible inverted basins in the RMFZ. Growth folding may accompany part or all of the compression that drives uplift. The Tolt Hill growth fold (Fig. 1, site 4) of Dragovich and others (2007) is interpreted to be one of a number of possible growth folds in the area. Tilted or folded Olympia beds are unconformably overlain by Vashon glacial deposits in many areas. For example, Olympia beds at critical site 13V (Plate 1) dip steeply to the southeast along an inferred fold axis and are overlain by gently dipping Vashon glaciofluvastirne deposits (Fig. 5 in appendix 5 of Dragovich and others 2009a).

Obtaining direct field evidence for Holocene motion on fault strands in the region is complicated by dense vegetative cover and urbanization. In lieu of trenching suspected fault traces, fault investigations must rely on sparse outcroppings near lineaments. Faults are mapped on the basis of our interpretation of geographic, geophysical (Figs. 3 and 4), geomorphic, and stratigraphic lineaments or anomalies, as well as our interpretation of deformational features observed in outcrop, both locally and regionally (Dragovich and others, 2007, 2009a,b). Also, some faults are aligned with buried bedrock escarpments or lineaments illustrated on Figure 2. We have queried faults where the evidence of faulting is indirect (for example, geophysical lineaments) and (or) the evidence for faulting is from poorly exposed outcrops near short or subtle lineaments visible on lidar. Long-term strike-slip fault movement on the RMFZ is indicated by outcrop structures, fault-strand linearity, its resemblance to a negative flower structure (for example, Fig. 4B), along-strike variation in structural features, and the occurrence of inverted, pull-apart basins. Quaternary activity along strands of the RMFZ is suggested by steeply dipping fractures, small faults, sand dikes, and other liquefaction features in Vashon glacial deposits and Olympia beds near these faults. (See critical sites noted in unit Qtz description on Plate 1 and sites 5 and 6 on Figure 1.) Tectonic faults, fractures, slickenlines, and associated liquefaction features—sand dikes and flame structures—differ from the soft-sediment deformation structures locally noted in advance lake and outwash deposits, resulting from ice shear (critical sites 1H, 33AG, 33M, 38L, 54N, 54Z, and 56Q, Plate 1). Ice-shear structures at these sites have a ductile-flow aspect and display recumbent folds and other structures resulting from low-angle simple shear. Some of these faults have been active in the Quaternary. Available information suggests that Rattlesnake Mountain faults (RMF) nos. 1, 6, 11, and perhaps 3 and 4, are active or have had Holocene displacement. Older Pleistocene displacement can be more firmly established for all these faults, particularly RMF nos. 1, 3, 4, and 11, on the basis of the deformational structures observed in the older Olympia beds in the Fall City, North Bend, and Snoqualmie 7.5-minute quadrangles (this study; Dragovich and others, 2007, 2009a, b).

Significant dip-slip motion on the Tokul Creek and Snoqualmie Valley faults is indicated by the westerly "stratigraphic younging" from pre-Tertiary to Eocene to Miocene across these faults. Miocene rocks are exposed at the surface west of the Snoqualmie Valley fault. The Griffin Creek fault is mapped along a wide lineament that is oblique to the glacial flutings and glacial striae. The lack of offset of flutes and smooth nature of this lineament suggest that this inferred fault zone is dormant. Although two short, subtle terraces visible on lidar in the north-central part of the quadrangle may be active fault scarps, we cannot rule out landsliding or latest Pleistocene to Holocene erosion as causes for these scarps. The Tokul Creek fault generally juxtaposes Western melange belt basement against Eocene volcanic rocks of Mount Persis (Fig. 3). This fault was mapped regionally by Tabor and others (1993)(Fig. 1) and could be a Cascade Range frontal fault accommodating Cascade Range uplift. The concentration of midcrustal to shallow earthquake hypocenters around the Tokul Creek fault and subparallel faults implies an active fault or subparallel faults; several hypocenters along the projection of these high-angle faults have left-lateral strike-slip focal mechanism solutions (Fig. 4). We call this family of north-northeast-trending faults the Tokul Creek fault zone. The Tokul or Griffin Creek faults may be implicated in the Tolt River earthquake, directly north of the map area (site 8, Fig. 1), described by Bradford and Waters (1934). The Snoqualmie Valley fault juxtaposes Eocene volcanic rocks of Mount Persis with younger Miocene to Oligocene volcanic (units Mvaᵦ and Mvtxᵦ) and marine rocks (unit ΦEn) indicating a long-term component of dip-slip or oblique-slip motion (Fig. 4). Some earthquake focal mechanisms near the Snoqualmie Valley and Griffin Creek fault strands have right-lateral strike-slip focal mechanism solutions; one of these faults may define the easternmost extent of the regional RMFZ–SWIF structure. Left-lateral and right-lateral strike-slip offset for the Tokul Creek and RMFZ, respectively, are consistent with a conjugate strike-slip fault model containing a north–south principal axis of stress.

Table 1. Radiocarbon age key for Cross Sections A and B. Cross section labels are ordered from left to right and relate age date symbols on the cross sections to those on the map. Symbols are either from a borehole site or horizontally projected from a surface sample site near the cross section line. For more details, see table 1 of Dragovich and others (2009a), which also discusses Olympia bed samples in the Fall City 7.5-minute quadrangle (Dragovich and others, 2007).

Cross section label	Boring or site no.	Radiocarbon age (yr B.P.)	Notes (sample elevation is ft above or below sea level)
1a	AES-2	41,270 ±1,610	Associated Earth Sciences (AES) unpublished radiocarbon age (J. Saltonstall, written commun., 2007); surface sample elevation ~955 ft; located 3,300 ft SSE of the west end of Cross Section A in unit Qcᵧ at age site AES-2 (Plate 1); organic sediment
2a	TW–1	24,750 ±980	Associated Earth Sciences (1987); sample elevation at ~270 ft; located near west end of Cross Section A in unit Qcᵧ
3a	TW–1	25,280 ±550	Associated Earth Sciences (1987); sample elevation at ~500 ft; located near west end of Cross Section A in unit Qcᵧ
4a	B289B	3,040 ±80	Associated Earth Sciences (1995); sample elevation at 392 ft; located near middle of Cross Section A in unit Qa
5a	W80	5,720 (no error reported)	GeoEngineers (1995); sample elevation at ~320 ft; projected ~5,600 ft north near middle of Cross Section A in unit Qa
6a	W80	>43,000	GeoEngineers (1995); sample elevation at ~ –51 ft; projected ~5,600 ft north near middle of Cross Section A in unit Qcᵧ
1b	TW–2	29,460 ±1,380	Associated Earth Sciences (1987); sample elevation at ~530 ft; located near west end of Cross Section B in unit Qcᵧ
2b	08–4M	45,540 ±930	This study; surface sample elevation at ~510 ft; located near the west end of Cross Section B in unit Qcᵧ, at age site 4M; may be "infinite"
3b	08–31L	>44,020	This study; surface sample elevation at ~495 ft; located in unit Qcᵧ at age site 31L (Plate 1) near Rattlesnake Mountain fault no. 1 on Cross Section B
4b	08–31C	>43,870	This study; surface sample elevation at ~555 ft; located in unit Qcᵧ at age site 31C (Plate 1) near Snoqualmie River on Cross Section B

GEOPHYSICAL ANALYSES OF THE MAP AREA

Magnetic and Gravity Anomaly Analyses

Aeromagnetic data comes from a survey contracted by the USGS in 1997. Flight lines are oriented north–south and have a 250-m spacing (Blakely and others, 1999). Magnetic anomalies for the map area are strongly asymmetric with respect to the source of the magnetic anomaly. Therefore, we present a reduced-to-pole aeromagnetic anomaly map, calculated using standard procedures (Blakely, 1995; Fig. 3A). This filter moves magnetic anomalies directly over the causative magnetic source units. We upward continue the reduced-to-pole magnetic grid to 50 m above the flight altitude and then subtract the product from our original magnetic grid. The resulting map isolates the anomalies produced by near-surface magnetic rocks. Recent data constrain the isostatic gravity anomalies for this region (Anderson and others, 2006). Standard formulas and reduction procedures (Blakely, 1995), as well as a reduction density of 2670 kg/m³ for the crust, constrain the isostatic gravity anomaly contours. Geophysical profile models were calculated with GM-SYS Geophysical Modeling software (NGA, Inc.). Sampling of the magnetic grid for the model profile is 250 m, similar to the spacing of flight lines on the aeromagnetic survey. Magnetic measurement altitudes in the profiles are matched to the airplane altitude recorded by radar altimeter during the aeromagnetic survey. Gravity constraint is considerably sparser—more on the order of a grid with a spacing of 1 km between stations in the southern half of the map and 3.5 km in the northern half (Fig. 3A). We only display gravity data points that lie within about 1 km of the profile lines. Therefore, some of the details on the profiles less than 1 km in width are based on geologic mapping, and though they match the existing gravity grid, are not constrained by the geophysics.

Density and magnetic properties of the rocks and rock units used in the two-dimensional geophysical modeling are supported by hand sample and outcrop magnetic susceptibility measurements, as well as hand sample density measurements (Anderson and others, 2006; Megan Anderson, unpub. data, 2006–2009). Geophysical properties of "combined" units are averaged from hand samples of each component, based on the percentage of each component exposed in outcrops in the area. For example, greenstone is estimated to compose about 15 percent of the Western mélange belt in the map area, an estimate that may be too high for the melange belt as a whole (R. W. Tabor, USGS emeritus, written commun., 2008), but makes the Western melange belt slightly denser than average in our study region. Most of the rock densities and magnetic susceptibilities of units closely follow those used for the North Bend quadrangle models (Dragovich and others, 2009b). However, the Tukwila Formation is significantly more magnetic in the models presented here, which may be admissible given the potential for this unit to contain more magnetically susceptible volcanic tuff breccias towards the west end of our models. This is supported by measurements on the Tukwila tuff breccias in the Fall City quadrangle directly to the west (Dragovich and others, 2007). Our modeling procedure honors both the mapped lithologic boundaries and the thickness of Quaternary sediments (Fig. 2) across the profiles. Deeper boundaries are based solely on the geophysical evidence and structural inference. Basement properties are based on modeling from areas farther to the west in the Puget Lowland (Anderson and others, 2006).

The strongest geophysical anomaly in the Snoqualmie quadrangle is created by the volcanic rocks of Rattlesnake Mountain (RS on Fig. 3A). This strong magnetic high results from a combination of north–south-striking fault-bounded wedge of magnetically susceptible volcanic rocks that forms the core of Rattlesnake Mountain (Dragovich and others, 2009b). Other magnetic rocks in the region include the younger volcanic rocks of Snoqualmie Falls (Fig. 3A, anomalies VSF1 and VSF2) and the volcanic rocks of Mount Persis (Fig. 3A, MP1 and MP?). The magma source for the volcanic rocks of Snoqualmie Falls, which are preserved in the Snoqualmie basin, was probably the Snoqualmie batholith. Magnetic and gravitational lows in the central-southwest portion of the map (Fig. 3A, SVB and RF) result from moderately magnetic to nonmagnetic rocks of the Renton Formation or the undivided Puget Group occupying RMFZ basins. Other magnetic lows on the map include (1) the area east of the Tokul Creek fault, due to the Western mélange belt rocks (Fig. 3A, WMB), and (2) sediments filling the north end of the North Bend basin (Fig. 3A, NBB). Thick Tertiary sediments may be responsible for the magnetic low along the northern border of the map (Fig. 3A, unit OEC?). Note that most faults mapped in the quadrangle track the edges of the different magnetic units and (or) gravitational anomalies, with the exception of the Griffin Creek fault. Therefore, based on the observation that the Mount Persis anomalies do not appear to be affected by the fault, we interpret the Griffin Creek fault to be either older than the volcanic rocks of Mount Persis or to possess little offset (perhaps because the fault is young).

Due to the complexity of the subsurface geology, there are many possible subsurface rock geometries that will fit our geophysical data. Cross Sections A and B were modified to fit most of the observed gravity and magnetic data. In addition, we attempt to constrain the range of plausible results by using densities and magnetic susceptibilities for most units that are similar to those used in the North Bend quadrangle (Dragovich and others, 2009b), where the geology is relatively simple and thus has more uniquely constrained physical properties. Our ability to geophysically determine the depth to the base of the volcanic rocks of Rattlesnake Mountain and the Tukwila Formation is strongly dependent on the magnetic properties of these rocks, which are variable; therefore, there is some uncertainty as to the thickness of these units. The volcanic rocks of Snoqualmie Falls require a very high magnetization to fit the magnetic anomaly (Fig. 3A, VSF1 and VSF2). Though a high magnetic susceptibility is supported by hand sample and outcrop measurements, lower overall magnetization is acceptable because it can be offset by a slightly thicker section or a slightly higher magnetization of the underlying Snoqualmie batholith.

Gravity is strongly influenced by thick pull-apart basin fill in the western half of both profiles (Fig. 3B–C). The Quaternary sediments, volcanic rocks of Snoqualmie Falls, and Blakeley Formation are likely basin fill; however, older Tertiary volcanic and sedimentary rocks may also fill early RMFZ subbasins. The thickness of sedimentary and volcanic rocks is more reliable on profile C–C′ than D–D′, because profile C–C′ trends perpendicular to the strike of anomaly boundaries. The thickness assigned to Quaternary deposits across each profile depends on the density of those deposits, which is variable, though the modeled depth generally matches depth to bedrock determinations (Fig. 2). Low-density cataclasite (unit tz) along the RMFZ (particularly RMF-1) is necessary in both profiles to fit the gravity, similar to results for the North Bend quadrangle (Dragovich and others, 2009b). Dips of fault-bounded blocks are less well-constrained in this model than in the North Bend study because of more complex relationships between packages of magnetic rocks; however, the position of fault-bounded rocks matches well with the initial determinations derived solely from structural-stratigraphic inferences in the geologic cross section models. There is one important adjustment to the cross section from the geophysical modeling: the edges of the undifferentiated Snoqualmie batholith. These boundaries strongly control the position of maximum gradients on the flanks of the aeromagnetic high in the middle of each profile. We found that putting strongly magnetic batholithic material either to the west of RMF-1 or to the east of the Snoqualmie Valley and Tokul Creek faults produced a poor fit of the aeromagnetic anomaly data. Therefore, we are comfortable with the faulted-boundary interpretation represented on the model profiles, and the Snoqualmie batholith may not reside at relatively shallow depth east of the Snoqualmie Valley fault or west of RMF-1 as implied by the geologic Cross Section B. We suspect that the undifferentiated batholith shown in the model is a mixture of gabbroic to granodioritic rock types. The gravity and magnetic properties used for these bodies generally have assigned values intermediate between these rock types. Basement and nonmagnetic parts of the Western mélange belt are nearly indistinguishable geophysically, and the exact location of the boundary between the two units is somewhat flexible; for these units, we used rock properties similar to those in the North Bend quadrangle (Dragovich and others, 2009b), where the boundary showed more prominently in the gravity data. Metagabbro at depth is postulated solely on the geophysics, as required to fit the data, though the metagabbro properties used in modeling follow measurements of only a few outcrops in the North Bend area. The magnetization of the Snoqualmie batholith gabbro is similar to the volcanic rocks of Snoqualmie Falls—not Snoqualmie batholith granodiorite—therefore, the magnetic data suggest that the underside of the volcanic rocks of Snoqualmie Falls is spatially associated with and may be derived from mafic Snoqualmie batholith magma.

Seismicity in the Map Area

To investigate the relation between modern seismicity and the location of mapped faults in the Snoqualmie quadrangle, earthquakes from the Pacific Northwest Seismic Network (PNSN) catalog (accessed March 2009) that occurred within the Snoqualmie quadrangle between 1980 and March 2009 have been relocated using the double-difference algorithm of Waldhauser and Ellsworth (2000). The algorithm uses the fact that ray paths from two earthquakes close to a common station are almost identical and the difference in observed travel time can therefore be attributed with a high degree of certainty to the spatial offset of the two earthquakes. We used analyst picks and did not re-pick arrival times. Furthermore, only three network stations are located close to the source region, and the accuracy of the earthquake locations is therefore limited, due both to station distribution and possible picking errors. To select earthquakes, we included only those events for which we have waveform data (to be able to verify quality of picks) and that had a duration magnitude (Md) of 1.0 or more. This resulted in 153 events, of which we were able to successfully relocate 133. (A total of 261 PNSN catalog earthquakes of variable size and quality occurred in the Snoqualmie 7.5-minute quadrangle from 1969 to 2008.) The largest event containing waveform data was an Md=2.9 event that occurred in northwestern part of the quadrangle. Only 23 shallow (depth <10 km) earthquakes were relocated in the quadrangle. The majority of the microearthquakes occur in a depth range of 10 to 18 km (96 out of our 133 relocated events)—shallower and deeper crustal earthquakes have been much less frequent. In the North Bend quadrangle (Dragovich and others, 2009b), midcrustal microearthquakes are concentrated in a slightly greater depth (28 km). First-motion focal mechanisms indicate mostly reverse faults and a few smaller areas where strike-slip mechanisms are common. In general, these earthquakes are consistent with north–south compression, which is thought to be the dominant mode of deformation in this region (Fig. 4A-D). How the midcrustal seismicity connects to shallower seismicity and mapped faults is difficult to determine, due to the small number of earthquakes. Therefore our stipulations concerning fault geometry using the earthquake data should be considered speculative (Figs. 4B-D). The correlation of individual fault strands mapped at the surface with hypocenters at depth depends upon the subsurface geometry of the faults, including the fault dip and curvature, which has many degrees of freedom and is poorly constrained. Fault dips can be estimated for the uppermost crust by combining the surface fault trace with possible fault dips inferred from our geophysical modeling (Figs. 3B-C). This combined dataset provides three first-order constraints on the geometry of some of the fault zones: (1) fault strands in the western RMFZ dip to the east, (2) fault strands near the main strand of the RMFZ (RMF-11) and Tokul Creek fault zone are subvertical, and (3) fault strands in the eastern RMFZ and along the Snoqualmie Valley fault dip to the west. Correlation of individual strands with individual hypocenters is partly driven by these general constraints and partly by our model of the RMFZ as a strike-slip fault zone containing a negative flower structure (see 'Tertiary to Quaternary Deformation in the Map Area—Faults, Basins, and Folds' and Dragovich and others [2009a]).

ACKNOWLEDGMENTS

This geologic map was funded in part by the U.S. Geological Survey (USGS) National Cooperative Geologic Mapping Program under award no. 08HQAG0104. We thank many people for assistance: Curtis Koger and Jennifer Saltonstall (Associated Earth Sciences, Inc.) for subsurface geotechnical information, unpublished radiocarbon ages, and information on unpublished anomalies, with the exception of the Griffin Creek fault; Jennifer Vanderburg (Univ. of Wash.) for identifying macrofossils; Linda Reinink-Smith and Estella Leopold (Univ. of Wash.) for analyzing sample pollen grains; Diane Cornelius, Rick Conrey, and Charles Knaack (Wash. State Univ.) for geochemical analyses of samples; Willis Littke (Weyerhaeuser Corp.) for field observations; Rowland Tabor (USGS emeritus) for geologic input. We thank James Johnson (Golder Associates), Russ Steele (Wash. Dept. of Transportation), Steve Bonheim (King County DDES), Sue Kahle and Myrtle Jones (USGS, Water Resources Division, Tacoma) for subsurface geologic information. We also thank Julie Stangell (Hancock Forest Management) for property access; Brian Ballard (Wash. Dept. of Natural Resources) for geological input; David Magnuson (Puget Sound Energy) for access to Snoqualmie Falls underground facilities; Cheryl Proffitt, Kenneth Hearing, and Duncan Wilson (City of North Bend) for house rental; Albert Gonzales and Mike Leathers (King County Information Technology Division, GIS Products and Services) for the lidar data. We thank the following Washington Division of Geology and Earth Resources colleagues: Josh Logan, Dave Norman, and Trevor Contreras for map and text reviews, Fritz Wolff for compiling subsurface information, Robert Berwick for metadata and file management, and Lee Walking for assistance with references.

REFERENCES CITED ON PLATES 1 AND 2

Anderson, M. L.; Blakely, R. J.; Brocher, T. M.; Pratt, T. L.; Wells, R. E.; Haugerud, R.; Bush, M., 2006, Structure of the Seattle uplift from seismic, gravity, magnetic, geologic, and geomorphic data: Eos (American Geophysics Union Transactions), v. 87, no. 52, Supplement, Abstract T41A-1554.

Armstrong, J. E.; Crandell, D. R.; Easterbrook, D. J.; Noble, J. B., 1965, Late Pleistocene stratigraphy and chronology in southwestern British Columbia and northwestern Washington: Geological Society of America Bulletin, v. 76, no. 3, p. 321-330.

Associated Earth Sciences, Inc., 1987, Snoqualmie Ridge project, King County, Washington—Soils, geology, geologic hazards and ground water hydrogeology: Associated Earth Sciences, Inc. [Kirkland, Wash., under contract to] Snoqualmie Ridge Associates, Inc., 2 v., 4 plates.

Associated Earth Sciences, Inc., 1995, Proposed Kimball Creek pump station, Snoqualmie, Washington—Seismic evaluation report, Snoqualmie WWTP project: Associated Earth Sciences, Inc. [prepared for KCM, Inc., project H95125D]. 1 v.

Associated Earth Sciences, Inc., 1996, Snoqualmie North Valley well field, Snoqualmie, Washington—Hydrogeologic evaluation for source approval of Group A public water systems WAC 246-290-130: Associated Earth Sciences, Inc., [prepared for Weyerhaeuser Real Estate Company, project W96078C]. 1 v.

Associated Earth Sciences, Inc., 2003, Proposed Snoqualmie Ridge II project—Environmental impact statement—Technical report on geology, soils, and groundwater: Associated Earth Sciences, Inc., [Kirkland, Wash., under contract to] Quadrant Corporation, 1 v.

Associated Earth Sciences, Inc., 2005, Proposed Snoqualmie Ridge II N1 and N2 infiltration ponds—Technical report on geology and groundwater: Associated Earth Sciences, Inc. [Kirkland, Wash., under contract to] Quadrant Corporation, 1 v.

Blakely, R. J., 1995, Potential theory in gravity and magnetic applications: Cambridge University Press, 441 p.

Blakely, R. J.; Wells, R. E.; Weaver, C. S., 1999, Puget Sound aeromagnetic maps and data: U.S. Geological Survey Open-File Report 99-514, version 1.0. [http://geopubs.wr.usgs.gov/open-file/of99-514/]

Booth, D. B., 1984, Glacier dynamics and the development of glacial landforms in the eastern Puget Lowland, Washington: University of Washington Doctor of Philosophy thesis, 217 p., 1 plate.

Booth, D. B., 1986, The formation of ice-marginal embankments into ice-dammed lakes in the eastern Puget Lowland, Washington, U.S.A., during the late Pleistocene: Boreas, v. 15, no. 3, p. 209-264.

Booth, D. B., 1990, Surficial geologic map of the Skykomish and Snoqualmie Rivers area, Snohomish and King Counties, Washington: U.S. Geological Survey Miscellaneous Investigations Series Map I-1745, 2 sheets, scale 1:50,000, with 22 p. text.

Bradford, D. C.; Waters, A. C., 1934, The Tolt River earthquake and its bearing on the structure of the Cascade Range: Seismological Society of America Bulletin, v. 24, no. 1, p. 51-62.

Dickinson, W. R., 1970, Interpreting detrital modes of greywacke and arkose: Journal of Sedimentary Petrology, v. 40, no. 2, p. 695-707.

Dragovich, J. D., 2007, Sand point count and geochemical data in the Fall City and Carnation 7.5-minute quadrangles, King County, Washington—Supplement to GM-64: Washington Division of Geology and Earth Resources Open File Report 2007-3, 2 Microsoft Excel files with 6 p. text. [http://www.dnr.wa.gov/Publications/ger_ofr2007-3_fallcity_supplement.zip]

Dragovich, J. D.; Anderson, M. L.; Walsh, T. J.; Johnson, B. L.; Adams, T. L., 2007, Geologic map of the Fall City 7.5-minute quadrangle, King County, Washington: Washington Division of Geology and Earth Resources Geologic Map GM-67, 1 sheet, scale 1:24,000. [http://www.dnr.wa.gov/Publications/ger_gm67_geol_map_fall city_24k.zip]

Dragovich, J. D.; Littke, H. A.; MacDonald, J. H., Jr.; DuFrane, S. A.; Anderson, M. L.; Wessel, G. R.; Hartog, Renate, 2009a, Geochemistry, geochronology, and sand point count data for the Snoqualmie 7.5-minute quadrangle, King County, Washington: Washington Division of Geology and Earth Resources Open File Report 2009-4, 3 Microsoft Excel files with 35 p. text. [http://www.dnr.wa.gov/Publications/ger_ofr2009-4_snoqualmie_geochem.zip]

Dragovich, J. D.; Logan, R. L.; Schasse, H. W.; Walsh, T. J.; Lingley, W. S., Jr.; Norman, D. K.; Gerstel, W. J.; Lapen, T. J.; Schuster, J. E.; Meyers, K. D., 2002, Geologic map of Washington—Northwest quadrant: Washington Division of Geology and Earth Resources Geologic Map GM-50, 3 sheets, scale 1:250,000, with 72 p. text.

Dragovich, J. D.; Walsh, T. J., 2008, Geochemical sample analyses of Tertiary and pre-Tertiary volcanic rocks in and around the North Bend 7.5-minute quadrangle, King County, Washington: Washington Division of Geology and Earth Resources Open File Report 2008-4, 1 Microsoft Excel file with 6 p. text. [http://www.dnr.wa.gov/Publications/ger_ofr2008-4_northbend_geochem.zip]

Dragovich, J. D.; Walsh, T. J.; Anderson, M. L.; Hartog, Renate; DuFrane, S. A.; Vervoot, Jeff; Williams, S. A.; Cakir, Recep; Stanton, K. D.; Wolff, F. E.; Norman, D. K.; Czajkowski, J. L., 2009b, Geologic map of the North Bend 7.5-minute quadrangle, King County, Washington, with a discussion of major faults, folds, and basins in the map area: Washington Division of Geology and Earth Resources Geologic Map GM-73, 1 sheet, scale 1:24,000, with 39 p. text. [http://www.dnr.wa.gov/Publications/ger_gm73_geol_map_northbend_24k.zip]

Erikson, E. H., Jr., 1969, Petrology of the composite Snoqualmie batholith, central Cascade mountains, Washington: Geological Society of America Bulletin, v. 80, no. 11, p. 2213-2236, 1 plate.

Fulmer, C. V., 1975, Stratigraphy and paleontology of the type Blakeley and Blakely Harbor Formations. *In* Weaver, V. M., Hornaday, G. R., Tipton, Anne, editors, Paleogene symposium and selected technical papers—Conference on future energy horizons of the Pacific coast: American Association of Petroleum Geologists Pacific Section, 50th Annual Meeting, p. 210-271.

GeoEngineers, Inc., 1995, Report of hydrogeologic services, south well field characterization, Snoqualmie, Washington: GeoEngineers [for Puget Western, Inc.], 1 v.

Jett, G. A., Heller, P. L., 1988, Tectonic significance of polymodal compositions in mélange sandstones, western mélange belt, north Cascade Range, Washington: Journal of Sedimentary Petrology, v. 58, no. 1, p. 52-61.

Jones, M. A., 1996, Thickness of unconsolidated deposits in the Puget Sound lowland, Washington and British Columbia: U.S. Geological Survey Water-Resources Investigations Report 94-4133, 1 sheet.

Klohn Cripper Berger, 2007, Snoqualmie Falls redevelopment project—2006 geotechnical investigations: Klohn Cripper Berger [for Puget Sound Energy Inc.], 1 v.

Le Maitre, R. W., ed., 2002, Igneous rocks—A classification and glossary of terms; 2nd ed.: Cambridge University Press [Cambridge, U.K.], 236 p.

Mackin, J. H., 1941, Glacial geology of the Snoqualmie–Cedar area, Washington: Journal of Geology, v. 49, no. 5, p. 449-481.

Marcus, K. L., 1981, The rocks of Bulson Creek—Eocene–Oligocene sedimentation and tectonics in the Lake McMurray area, Washington: Western Washington University Master of Science thesis, 84 p., 1 plate.

Minard, J. P.; Booth, D. B., 1988, Geologic map of the Redmond quadrangle, King County, Washington: U.S. Geological Survey Miscellaneous Field Studies Map MF-2016, 1 sheet, scale 1:24,000.

Pettijohn, F. J., 1957, Sedimentary rocks; 2nd ed.: Harper & Brothers, 718 p.

Porter, S. C.; Swanson, T. W., 1998, Radiocarbon age constraints on rates of advance and retreat of the Puget lobe of the Cordilleran ice sheet during the last glaciation: Quaternary Research, v. 50, no. 3, p. 205-213.

Sherrod, B. L.; Blakely, R. J.; Weaver, C. S.; Kelsey, H. M.; Barnett, Elizabeth; Liberty, Lee; Meagher, K. L.; Pape, Kristin, 2008, Finding concealed active faults—Extending the Southern Whidbey Island fault across the Puget Lowland, Washington: Journal of Geophysical Research, v. 113, B05313, doi:10.1029/2007JB005060, 2008.

Tabor, R. W.; Frizzell, V. A., Jr.; Booth, D. B.; Waitt, R. B., 2000, Geologic map of the Snoqualmie Pass 30 x 60 minute quadrangle, Washington: U.S. Geological Survey Geologic Investigations Series Map I-2538, 1 sheet, scale 1:100,000, with 27 p. text. [http://geopubs.wr.usgs.gov/i-map/i2538/]

Tabor, R. W.; Frizzell, V. A., Jr.; Booth, D. B.; Waitt, R. B.; Whetten, J. T.; Zartman, R. E., 1993, Geologic map of the Skykomish River 30- by 60-minute quadrangle, Washington: U.S. Geological Survey Miscellaneous Investigations Series Map I-1963, 1 sheet, scale 1:100,000, with 42 p. text.

Turner, D. L.; Frizzell, V. A., Jr.; Triplehorn, D. M.; Naeser, C. W., 1983, Radiometric dating of ash partings in coal of the Eocene Puget Group, Washington—Implications for paleobotanical stages: Geology, v. 11, no. 9, p. 527-531.

U.S. Geological Survey Geologic Names Committee, 2007, Divisions of geologic time—Major chronostratigraphic and geochronologic units: U.S. Geological Survey Fact Sheet 2007-3015, 2 p.

Vine, J. D., 1969, Geology and coal resources of the Cumberland, Hobart, and Maple Valley quadrangles, King County, Washington: U.S. Geological Survey Professional Paper 624, 67 p., 4 plates.

Waldhauser, F.; Ellsworth, W. L., 2000, A double-difference earthquake location algorithm—Method and application to the northern Hayward fault: Bulletin of the Seismological Society of America, v. 90, no. 6, p. 1353-1368.

Walsh, T. J., 1984, Geology and coal resources of central King County, Washington: Washington Division of Geology and Earth Resources Open File Report 84-3, 24 p., 2 plates.

Walsh, T. J.; Phillips, W. M., 1982, Coal rank and thermal maturation in King County, Washington: Washington Geologic Newsletter, v. 10, no. 1, p. 9-19.

Washington Oil World, 1930, Oil in water well excites Snoqualmie: Washington Oil World, v. 1, no. 16, p. 4.

Wolfe, J. A., 1968, Paleogene biostratigraphy of nonmarine rocks in King County, Washington: U.S. Geological Survey Professional Paper 571, 33 p., 7 plates.

Wolfe, J. A.; Forest, C. E.; Molnar, Peter, 1998, Paleobotanical evidence of Eocene and Oligocene paleoaltitudes in midlatitude western North America: Geological Society of America Bulletin, v. 110, no. 5, p. 664-678. ■

CROSS SECTION EXPLANATION

- Fault—dashed where inferred; queried where uncertain
- Qls — Ticks showing extent of surficial geologic units too thin to show at scale as polygons
- Relative fault movement away from viewer
- Relative fault movement toward viewer
- Relative fault movement in plane of cross section
- 1a. 41.2 ka — Radiocarbon age date projected onto cross section; see Table 1 for age date information
- Water well or boring
- *See 'Description of Map Units' on Plate 1 for unit descriptions*

CROSS SECTION MODELS

We examined ~575 wells, ~300 geotechnical borings, and ~325 test pit logs from various sources. We show a composite well (multiple borings at one point on the map) where well and boring locations are closely spaced and (or) where subsurface geologic conditions are consistent. Radiocarbon ages shown on the cross sections and Table 1 are further described in Dragovich and others (2009a). The bedrock top contour map (Fig 2) is generally consistent with Cross Sections A and B. However, bedrock top elevations shown on the cross sections may slightly diverge from our bedrock top elevation map due to the addition of new information to Figure 2 just before publication (Curtis Koger and Jenny Saltonstall, AESI, written commun., 2009). Although other solutions are possible, our geophysical model (Fig. 3) of the Snoqualmie basin is consistent with the stratigraphic arrangement we postulate. Relocated hypocenters near Cross Section A are shown on Figure 4B. The Western mélange belt (WMB) pre-Tertiary basement was mapped as far west as Rattlesnake Mountain fault no. 6 (RMF-6) in the North Bend quadrangle as well as the southern part of the map area (Plate 1). RMF-6 splays into RMF-11 south of the cross sections and thus RMF-11 represents the western edge of the WMB in both cross sections. North of the cross sections, RMF-11 splays into the RMFZ main strand (RMF-11) and thus RMF-1 defines the edge of the WMB along the west-central portion of the map area consistent with subsurface mapping in the adjacent Fall City quadrangle (Dragovich and others, 2007). The lower part of unit Qgᵢ, may contain some older deposits. The extent and thickness of the Renton Formation (unit Eᵣ) mapped in the subsurface east of RMF-3 is poorly constrained. Renton strata east of this fault should be considered undivided Puget Group and may include any Puget Group formation of relatively low magnetic susceptibility, such as the Renton or Tiger Mountain Formations or volcanic sedimentary rocks of the Tukwila Formation. The lower part of unit Evs on the cross sections may contain some Tiger Mountain Formation interbeds. Geologic cross section lines are shown on Figures 2 and 3A. Major sources of subsurface data include Associated Earth Sciences (1987, 2003) and Klohn Cripper Berger (2007).

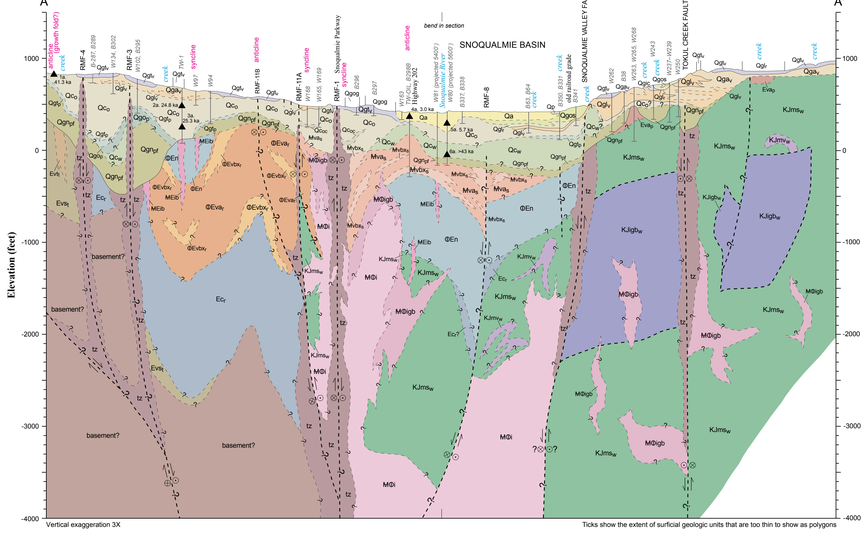

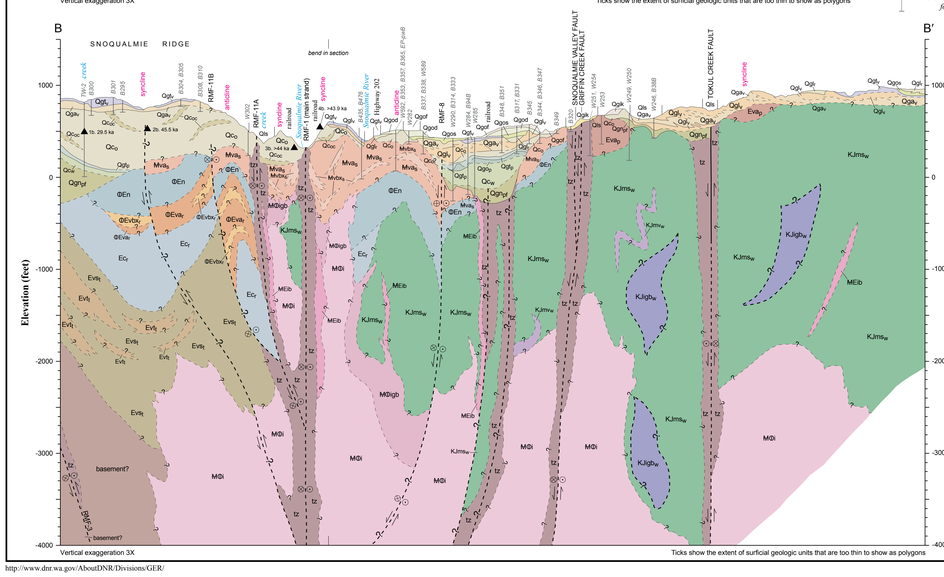

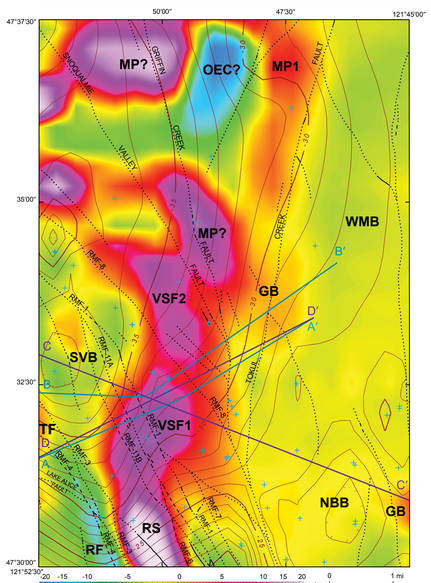

Figure 3A. Gravity and aeromagnetic map of the Snoqualmie 7.5-minute quadrangle with isostatic gravity anomaly contours (Anderson and others, 2006) superimposed on the aeromagnetic anomaly map (Blakely and others, 1999). Note: fault symbology simplified from geologic map (Plate 1) for clarity. **GB**, metagabbro; **MP**, volcanic rocks of Mount Persis; **NBB**, North Bend basin; **OEC**, undifferentiated continental sedimentary rocks; **RF**, Renton Formation; **RMF**, Rattlesnake Mountain fault; **RS**, volcanic rocks of Rattlesnake Mountain; **SVB**, Snoqualmie valley basin; **SVF**, Snoqualmie Valley fault; **TCF**, Tokul Creek fault; **TF**, Tukwila Formation; **VSF**, volcanic rocks of Snoqualmie Falls; **WMB**, Western mélange belt.

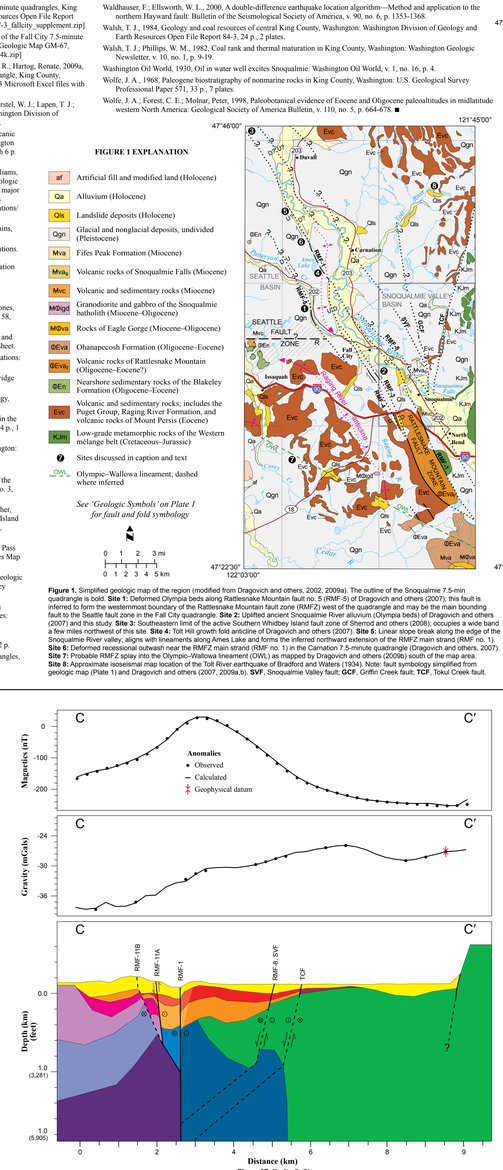
FIGURE 2 EXPLANATION
Anc